Extended abstract for the I3RC workshop, Tucson, Arizona, November 17–19, 1999

I3RC phase 1 results from the MYSTIC Monte Carlo model

Bernhard Mayer

National Center for Atmospheric Research (NCAR), Boulder, Colorado.

Abstract. This article provides a complete description of the radiative transfer model used in the I3RC (Intercomparison of 3D Radiation Codes) campaign. The MYSTIC model is a forward photon tracing method which solves the equation of radiative transfer for the specified conditions without any simplifying assumptions, simulating the involved physics as closely as possible. The methodology used to calculate the requested parameters is described in detail, and some sample results are presented.

1. Model description

The Monte Carlo model used for this study (MYSTIC[1]) is a forward photon tracing method, similar to those described by *Cahalan et al.* [1994] and *O'Hirok and Gautier* [1998]. In addition to three-dimensional atmospheres, it allows the realistic treatment of inhomogeneous surface albedo and topography, see e.g. *Kylling et al.* [1999]. The model atmosphere consists of a 1D background of molecules and aerosol particles and a 3D grid of cloud cells. See Figure 1 for a simple example.

[1]MYSTIC: Monte carlo code for the phYSically correct Tracing of photons In Cloudy atmospheres.

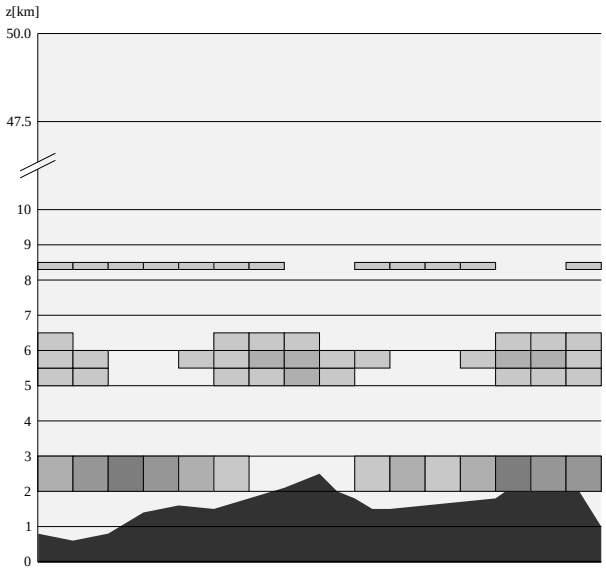

Figure 1. A simple example of the atmosphere used as input to the MYSTIC model (2D cross section of a 3D geometry). Rayleigh and aerosol scattering as well as molecular absorption are described by the 1D background atmosphere. Embedded are three layers of clouds, over some mountainous terrain.

A schematic diagram of the algorithm is shown in Figure 2. The involved physics is simulated as closely as possible on the basis of the input atmosphere, without any further simplifying assumptions. All processes involving random numbers are marked with a double-frame. The r250 algorithm of *Kirkpatrick and Stoll* [1981] was chosen as random number generator. Photons start at the top of the atmosphere (TOA) and travel from one scattering event to the next where the length of each path segment is determined by the scattering coefficient, $\beta_{\rm sca}$, and the direction (θ, ϕ) by the phase function $p(\theta)$. At the start and after each scattering event, the photon is assigned an optical depth $\Delta\tau_{sca}$ which it travels before the next scattering. The probability p that a photon is traveling the optical depth $\Delta\tau_{\rm sca}$ without being scattered is given by Lambert-Beer's law, $p = \exp(-\Delta\tau_{\rm sca})$. Using the cumulative probility function, $P(\tau) = \int_0^\tau p(\tau')d\tau' = 1-\exp(-\tau)$, the length of an individual path segment $\Delta\tau_{sca}$ is calculated according to

$$\Delta\tau_{sca} = -\ln\rho \qquad (1)$$

where ρ is a random number between 0 and 1. This path segment is then translated from optical depth space to physical space, by integrating the scattering coeffcient $\beta_{\rm sca}$ along the photon path through as many grid boxes until $\Delta\tau_{sca}$ is reached. Here, periodic boundaries were applied; that is, photons leaving the model domain at one side, re-entered it at the opposite side.

At the end of each step – if the photon has not reached the Earth's surface or left at TOA – a new direction is determined according to the scattering properties at the new location. Scattering by molecules, aerosol particles, and cloud droplets is treated separately, assuming the Rayleigh phase function for molecular scattering, the Henyey-Greenstein (HG) phase function for aerosol scattering, and a HG or arbitrary phase function for cloud scattering. For the Rayleigh and HG phase functions, $p_{\rm Rayleigh}(\theta)$ and $p_{\rm HG}(\theta)$, the new direction is calculated analytically by evaluating the cumu-

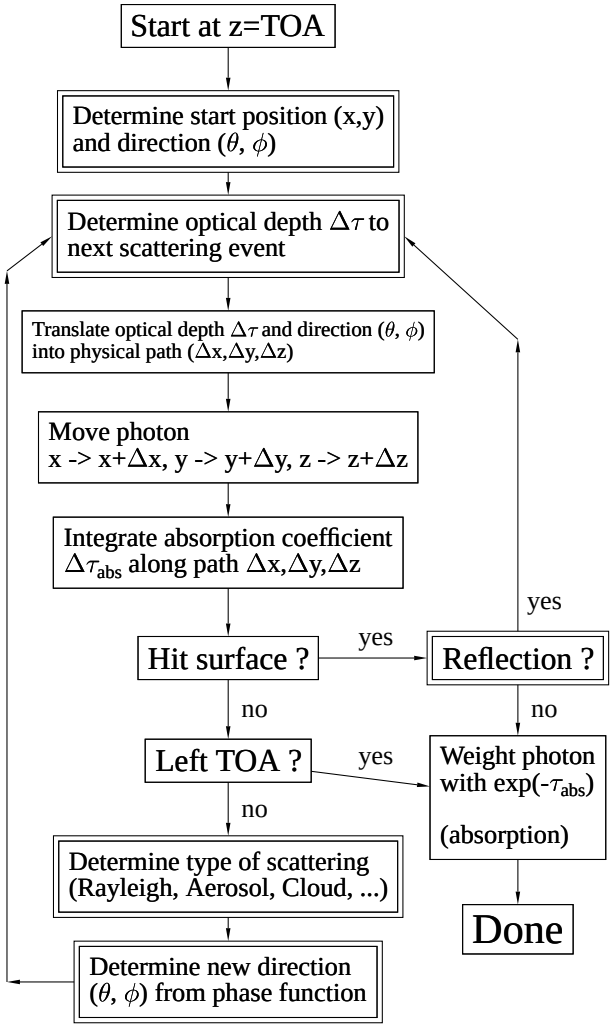

Figure 2. Schematic overview of the MYSTIC model. The double-framed boxes include a random number generation process.

lative probability functions, $P_{\mathrm{Rayleigh}}(\theta)$ and $P_{\mathrm{HG}}(\theta)$:

$$p_{\mathrm{Rayleigh}}(\theta) = \frac{3}{4}\left(1+\cos^2\theta\right) \quad (2)$$

$$p_{\mathrm{HG}}(\theta) = \frac{1-g^2}{(1+g^2-2g\cos\theta)^{\frac{3}{2}}} \quad (3)$$

where the asymmetry parameter g is typically about 0.85 for water clouds. Integrating these phase functions over θ to get the cumulative probability functions, and solving them for the scattering angle θ yields

$$\cos\theta_{\mathrm{Rayleigh}} = u - \tfrac{1}{u} \quad (4)$$
$$\text{with } u = \sqrt[3]{-q+\sqrt{1+q^2}}$$
$$\text{and } q = 4\rho - 2$$

for the Rayleigh scattering angle $\theta_{\mathrm{Rayleigh}}$ and

$$\cos\theta_{\mathrm{HG}} = \frac{1}{2g}\left[1+g^2-\left(\frac{g^2-1}{2g\rho-g-1}\right)^2\right] \quad (5)$$

for the HG scattering angle θ_{HG}, where ρ is a random number between 0 and 1. Other phase functions like the C1 phase function used for I3RC, which are defined at discrete points rather than analytically, are handled following the suggestion of *Barkstrom* [1995]: a table of the cumulative probability distribution is calculated from the moments of the phase function at 100,000 discrete, equidistant values of $\mu = \cos\theta$. The C1 phase function in I3RC was parameterized by its first 300 Legendre coefficients. The azimuth angle ϕ is assigned a random number between 0 and 2π, relative to a random direction. This process is repeated until a photon reaches the ground or leaves the atmosphere through TOA. At the surface, the photon is reflected into a random direction (assuming Lambertian reflection) with a probability given by the surface albedo A_{S}. Absorption is treated separately after the photon finished its path: for each step between two scattering events, the absorption coefficient, β_{abs}, is integrated over the respective path segment to yield the total absorption optical depth, τ_{abs} along the photon path. At the end of its path through the atmosphere, each photon is weighted with the Lambert-Beer factor, $\exp(-\tau_{\mathrm{abs}})$. Finally, the irradiance is the ratio of the sum of the Lambert-Beer factors of each photon reaching the surface and the number of photons incident at TOA, multiplied by the incident irradiance (the extraterrestrial irradiance multiplied with the cosine of the solar zenith angle). An important feature of MYSTIC is strict energy conservation, that is, for the I3RC cases, the sum of transmittance, albedo, and absorptance equals 1 exactly.

MYSTIC has been interfaced to the freely available libRadtran/uvspec model (see e.g. *Kylling et al.* [1999] and *Mayer et al.* [1997]) as well as to the tropospheric ultraviolet visible (TUV) model [*Madronich and Flocke*, 1997]. These are used to set up the optical properties of the atmosphere and to process the results to provide spectra, weighted doses, or photolysis frequencies. Standard output parameters include irradiance and actinic flux at specified altitudes

(split into their direct, diffuse-up, and diffuse-down components), the absorption for all grid cells, as well as radiances at specified directions and altitudes. In addition to a three-dimensional description of the atmosphere, the model is capable of handling inhomogeneous surface albedo and topography. The surface altitude $h(x, y)$ is defined on a rectangular grid. In between it is interpolated bi-linearly, $h(x, y) = ax + by + cxy + d$. Lambertian reflection off the inclined surfaces is considered correctly.

It should be emphasized that the MYSTIC model does not use any simplifying assumptions. Photons are traced until they either leave TOA or are absorbed at the surface. No biasing techniques are applied. The model accuracy is therefore determined only by the number of photons. The standard deviation of the result is proportional to the inverse square root of the number of photons traced. Comparisons of one-dimensional geometries using 10^9 photons have shown agreement with the DISORT code of *Stamnes et al.* [1988] within the MYSTIC statistical uncertainty of less than 0.01%.

The uncertainty of the result can be estimated a-priori. By simple statistics, it can be shown that the relative standard deviation σ of the result is (see e.g. *Cahalan et al.* [1994])

$$\sigma = \sqrt{\frac{N_0 - N_c}{N_0 N_c}} \tag{6}$$

where N_0 is the number of photons started at TOA and N_c is the number of photos sampled. As an example, if $N_c = 20000$ of the initial $N_0 = 10^6$ photons were sampled into the radiance at a certain point and angle, the uncertainty of this quantity will be $\sigma = 0.7\%$. For $N_c \ll N_0$, the relative uncertainty is defined by Poisson statistics, $\sigma = 1/\sqrt{N_c}$. It is important to note that N_c here refers to the number of photons before absorption (remembering that absorption is treated afterwards by applying a Lambert-Beer weighting factor). Thus, even in wavelength regions with high absorption, like the UV-B (280-315 nm), reasonable accuracy can be reached.

The Monte Carlo solver is written in ANSI C, optimized for being run on small machines. The calculations for I3RC, including the Landsat case with about 1,500,000 individual pixels, have been performed on an INTEL Pentium II / 350 MHz with 64 MBytes of memory. The computational speed was about 0.0003 seconds per photon for the step_cloud case, and 0.001 seconds per photon for the MMCR and Landsat cases.

2. Application in I3RC

The atmospheres for the step_cloud and MMCR cases were modelled exactly as defined. For the Landsat case, the cloud top altitudes were re-sampled on a 20 m vertical grid, resulting in a 1,500,000 pixel atmosphere. Due to this discretization, a maximum error of 10 m in the cloud top altitude is possible.

The computational time for the I3RC calculations is determined by the accuracy limits for the radiance calculations. A cone of 5° half opening angle was used for these, requiring about 10^8 photons to be traced for each experiment. For the MMCR and the Landsat cases, 10^8 photons were traced, while for the step_cloud this number was increased to 10^9 photons to reach even higher precision, see Table 1.

The pixel level errors are of course larger because less photons are sampled on each individual pixel. A rough estimate for the mean pixel level error is the number provided in Table 1, multiplied by the square root of the number of horizontal pixels: $\sqrt{32} \approx 5.7$ for step_cloud, $\sqrt{640} \approx 25$ for MMCR, and $\sqrt{16384} = 128$ for Landsat.

To calculate the statistical uncertainties, photons were started in packages of 10^6, and the errors were calculated from the standard deviation of the individual packages. E.g. the mean transmittance $\overline{T}$ and the percentage uncertainty of the mean transmittance, ΔT, were calculated as

$$\overline{T} = \sum_{i=1}^{N} T_i \tag{7}$$

$$\Delta T = \frac{100\%}{\overline{T}} \cdot \frac{1}{\sqrt{N}} \sqrt{\frac{1}{N} \sum_{i=1}^{N} (T_i - \overline{T})^2} \tag{8}$$

where T_i is an individual result for 10^6 photons and N is the number of 10^6-photon packages. The mean percentage pixel level error $\overline{\Delta T_p}$ was calculated as average over all individual pixel level errors $\Delta T_{p,j}$:

$$\Delta T_{p,j} = \frac{100\%}{\left| \overline{T_j} \right|} \cdot \frac{1}{\sqrt{N}} \sqrt{\frac{1}{N} \sum_{i=1}^{N} (T_{i,j} - \overline{T_j})^2} \tag{9}$$

$$\overline{\Delta T_p} = \frac{1}{N_{\mathrm{pixel}}} \sum_{j=1}^{N_{\mathrm{pixel}}} \Delta T_{p,j} \tag{10}$$

where $\overline{T_j}$ is the average transmittance for pixel j and N_{pixel} is the number of pixels. Only these pixels are counted into the average, where $\overline{T_j}$ was not 0.[2]

3. Results

Sample results for two cases are shown in Figures 3 and 4. Figure 3 shows as an example the first case, step_cloud, experiment 1 (solar zenith angle 0°, single scattering albedo $\omega = 1.0$). The number of photons traced, 10^9 is large enough to produce smooth curves even for the radiances. The mean pixel-level error is 0.03% for the transmittance and 0.5% for the nadir reflectivity. The transmittance through the center of the optically thinner part of the cloud (50 m $< x <$ 200 m) is larger than 1, indicating a strong net horizontal flux into this region. As expected for overhead sun, the I602 oblique reflectivity is the mirror image of the I601 reflectivity, mirrored at the center of the cloud cells at x=125 m or x=375 m.

[2] Pixels with $\overline{T_j} = 0$ occur e.g. for the nadir reflectivity in the Landsat case over cloudless areas.

Table 1. Number of photons used for I3RC and the resulting uncertainties.

Case	# of photons	error of the mean transmittance [%] [a]	error of the mean nadir reflectivity [%] [a]
step_cloud	10^9	0.004	0.07
MMCR	10^8	0.007	0.15
Landsat	10^8	0.013	0.22

[a]These values are 1 standard deviation, averaged over all experiments.

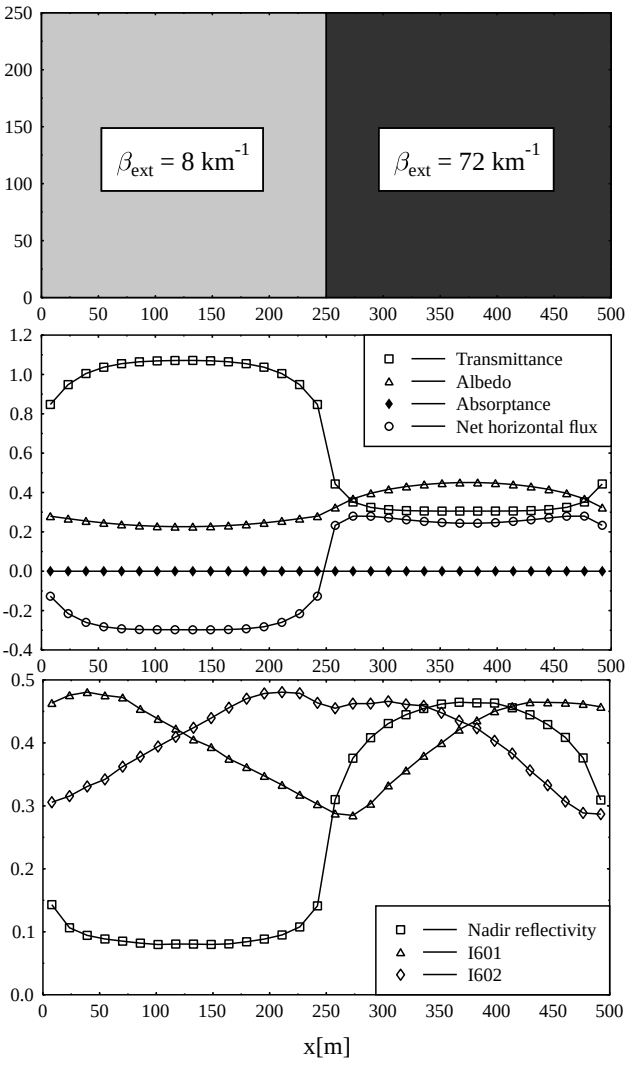

Figure 3. Result for the step_cloud case, experiment 1 (solar zenith angle $\theta = 0°$, single scattering albedo $\omega = 1.0$).

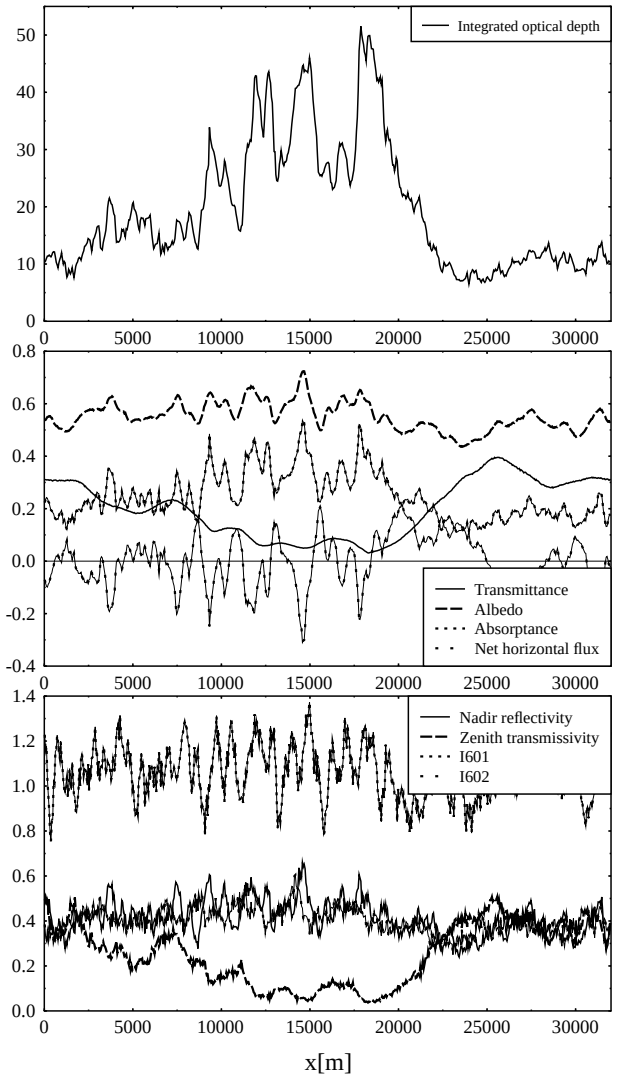

Figure 4. Result for the MMCR case, experiment 4 (solar zenith angle $\theta = 60°$, single scattering albedo $\omega = 0.99$).

Figure 4 shows a result for the second case, MMCR, experiment 4 (solar zenith angle 60°, single scattering albedo $\omega = 0.99$). Here, the number of photons traced, 10^8, is sufficient to reach the specified accuracy limits for the mean quantities. Due to the higher horizontal resolution and the smaller number of photons traced, however, some noise is introduced into the radiance distributions. The mean pixel-level errors are 0.3% for the transmittance and 4% for the nadir reflectivity. While albedo and absorptance show pronounced features correlating to the optical depth distribution, the transmittance is less structured, due to 'radiative smoothing'. Although not directly requested by I3RC, it is interesting to look at the oblique reflectivities I601 and I602. Due to the solar zenith angle of 60°, the symmetry between them is broken. The pronounced forward scattering by the cloud (asymmetry parameter g=0.85) causes the radiance reflected in the forward direction (I601) to be much higher (by a factor of about 2.5) than the backscattered radiance (I602).

Figure 5 shows a result for the third case, Landsat, experiment 3 (solar zenith angle 0°, single scattering albedo $\omega = 0.99$). The structures of the optical depth (top) are clearly visible in the nadir reflectivity (bottom). The albedo, however, shows a much smoother distribution due to the angular integration. This is most obvious over the cloudless areas in the corners of the field, where the nadir reflectance is of course 0 but the albedo is considerable, due to reflection off clouds to the sides. However, to interpret these figures, it has to be considered that the uncertainties are quite high, due to the large number of horizontal pixels (16384): while the mean pixel-level uncertainty of the albedo is still only 2.4%, the mean pixel-level uncertainty of the nadir reflectivity reaches 39%. Although this causes a grainy structure in the picture, the overall distribution is still visible and shows a high correlation with the optical depth. To improve this uncertainty to e.g. 4%, 100 times more photons would be required with the forward model, which would lead to unreasonable computational times with the current setup.

Finally, the 3D results were compared with independent pixel calculations by the DISORT discrete ordinate model of *Stamnes et al.* [1988]. The latter was operated in 16-streams mode with δ-M scaling. A comparison of the transmittance T, albedo R, absorptance A, and the nadir reflectivity Iu calculated with both methods is shown in Table 2. The best agreement between 3D and IPA was found for the MMCR case, where deviations were smaller than 1% for the transmittance, albedo, and absorptance. The differences are considerably higher in the step_cloud case, where the 3D transmittance is lower by 25% than its independent pixel approximation in experiment 4. The differences are larger at 60^o SZA than at overhead sun in both, the step_cloud and the Landsat cases.

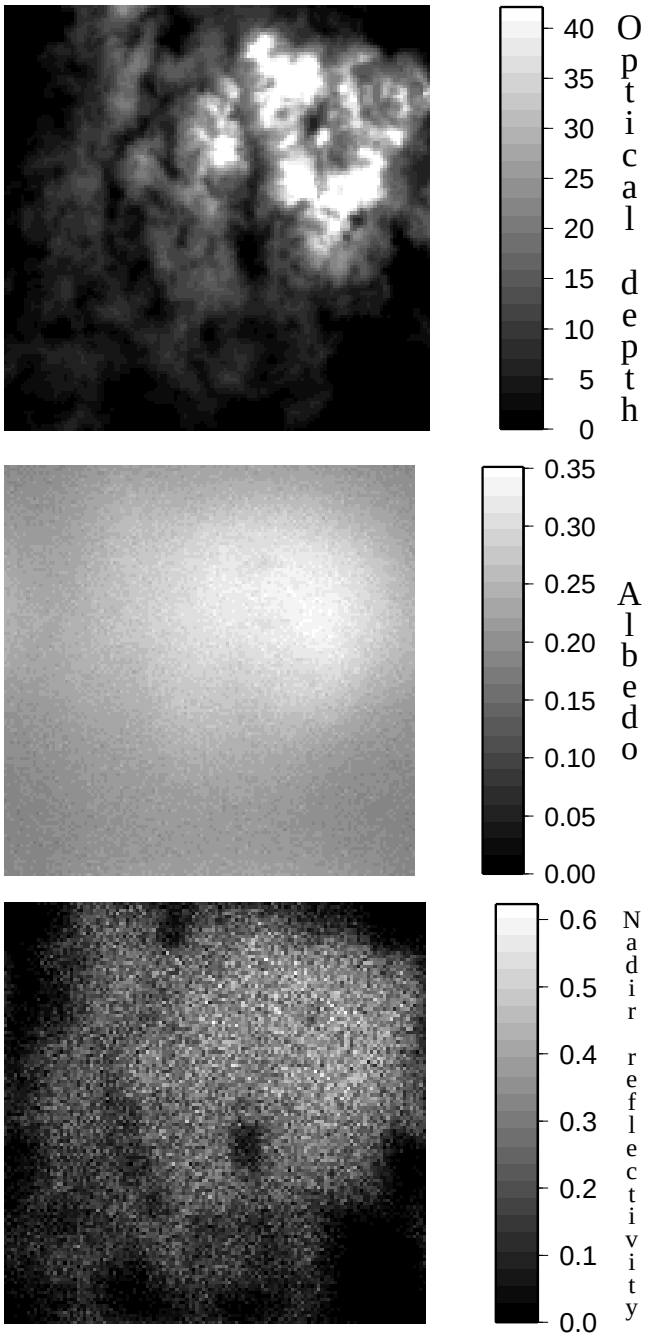

Figure 5. Result for the Landsat case, experiment 3 (solar zenith angle $\theta = 0°$, single scattering albedo $\omega = 0.99$).

4. Conclusions

Phase 1 of I3RC was a test of monochromatic radiative transfer through clouds in an otherwise empty atmosphere. The well-defined setup should help to identify reasons of possible discrepancies between different models. For the

Table 2. MYSTIC 3D and DISORT independent pixel (IPA) results.

Case	Exp.	T (3D)[a]	T (IPA)	R (3D)[a]	R (IPA)	A (3D)[a]	A (IPA)	Iu (3D)[a]	Iu (IPA)
step_cloud	1	0.67213	0.65979	0.32787	0.34019	0.00000	0.00002	0.2568	0.3158
step_cloud	2	0.41920	0.50018	0.58080	0.49979	0.00000	0.00003	0.4069	0.3567
step_cloud	3	0.59793	0.57656	0.26111	0.25840	0.14096	0.16504	0.2015	0.2265
step_cloud	4	0.32473	0.43065	0.47666	0.41840	0.19861	0.15095	0.3231	0.2779
MMCR	1	0.43987	0.43932	0.56014	0.56061	0.00000	0.00007	0.5685	0.5596
MMCR	2	0.30202	0.30090	0.69798	0.69904	0.00000	0.00006	0.5633	-
MMCR	3	0.30656	0.30690	0.40245	0.40327	0.29100	0.28983	0.3923	0.3835
MMCR	4	0.20033	0.20032	0.55200	0.55444	0.24767	0.24524	0.4137	-
MMCR	5	0.40376	0.40110	0.75785	0.75928	0.00000	0.00007	0.6399	-
MMCR	6	0.43798	-	0.56202	-	0.00000	-	0.6645	-
MMCR	7	0.29805	-	0.70195	-	0.00000	-	0.5271	-
MMCR	8	0.39916	-	0.76060	-	0.00000	-	0.6020	-
Landsat	1	0.69526	0.67445	0.30474	0.32549	0.00000	0.00006	0.2171	0.2994
Landsat	2	0.48521	0.52844	0.51479	0.47152	0.00000	0.00005	0.3332	-
Landsat	3	0.62770	0.59799	0.24256	0.24856	0.12974	0.15346	0.1709	0.2165
Landsat	4	0.40448	0.46415	0.42446	0.39363	0.17106	0.14222	0.2694	-

[a]T: transmittance; R: albedo; A: absorptance; Iu: nadir reflectivity.

next phases it would be interesting to also (1) compare results of the integrated shortwave irradiance; and (2) to add a background atmosphere with molecular and aerosol scattering and absorption.

The uvspec radiative transfer model used to drive the MYSTIC solver is part of the libRadtran package which is available from http://www.libradtran.org. The TUV radiative transfer model is available from http://acd.ucar.edu/UV/.

Acknowledgments. We would like to thank the I3RC team for the opportunity to participate in this very beneficial and well-organized campaign. Thanks to Sasha Madronich, Arve Kylling, and Edeltraud Leibrock for valuable discussion and comments on this manuscript. Special thanks to Edeltraud Leibrock for helping out with her Notebook to finalize the calculations. B.M. was supported by a research grant by the German Academic Exchange Service (DAAD). NCAR is sponsored by the National Science Foundation.

References

Barkstrom, B., An efficient algorithm for choosing scattering directions in Monte Carlo work with arbitrary phase functions, *J. Quant. Spectrosc. Radiat. Transfer*, *53*, 23–38, 1995.

Cahalan, R., W. Ridgway, W. Wiscombe, S. Gollmer, and Harshvardhan, Independent pixel and Monte Carlo estimates of stratocumulus albedo, *Journal of the Atmospheric Sciences*, *51*, 3776–3790, 1994.

Kirkpatrick, S., and E. Stoll, A very fast shift-register sequence random number generator, *Journal of Computational Physics*, *40*, 517–526, 1981.

Kylling, A., T. Persen, B. Mayer, and T. Svenoe, Determination of an effective spectral surface albedo from ground based global and direct UV irradiance measurements, *Journal of Geophysical Research*, 1999, in press.

Madronich, S., and S. Flocke, *Solar Ultraviolet Radiation. Modelling, Measurements and Effects*, vol. I52 of *NATO ASI*, chap. Theoretical estimation of biologically effective UV radiation at the Earth's surface, Springer-Verlag Berlin, Heidelberg, 1997.

Mayer, B., G. Seckmeyer, and A. Kylling, Systematic long-term comparison of spectral UV measurements and UVSPEC modeling results, *Journal of Geophysical Research*, *102*, 8755–8767, 1997.

O'Hirok, W., and C. Gautier, A three-dimensional radiative transfer model to investigate the solar radiation within a cloudy atmosphere. Part I: Spatial effects, *Journal of the Atmospheric Sciences*, *55*, 2162–2179, 1998.

Stamnes, K., S. Tsay, W. Wiscombe, and K. Jayaweera, A Numerically Stable Algorithm for Discrete-Ordinate-Method Radiative Transfer in Multiple Scattering and Emitting Layered Media, *Applied Optics*, *27*, 2502–2509, 1988.

B. Mayer, National Center for Atmospheric Research (NCAR), P.O. Box 3000, Boulder, CO 80307. (e-mail: bmayer@ucar.edu)

This preprint was prepared with AGU's LaTeX macros v4, with the extension package 'AGU++' by P. W. Daly, version 1.5e from 1997/11/18.